Progress In Electromagnetics Research, Vol. 138, 197–209, 2013

LOOP SWITCHING TECHNIQUE FOR WIRELESS POWER TRANSFER USING MAGNETIC RESONANCE COUPLING

Jungsik Kim, Won-Seok Choi, and Jinho Jeong*

Department of Electronic Engineering, Sogang University, Sinsu-dong 1, Mapo-gu, Seoul 121-742, Korea

Abstract—We propose a loop switching technique to improve the efficiency of wireless power transfer (WPT) systems using magnetic resonance coupling. The proposed system employs several loops with different sizes, one of which is connected to the system with various distances between the transmitter and the receiver. It enables the coupling coefficient to be adjusted with the distance, which allows high efficiency over a wide range of distances. The proposed system is analyzed using an equivalent circuit model, and electromagnetic (EM) simulation is performed to predict the performance. It is shown from the experimental results at 13.56 MHz that the proposed loop switching technique can maintain high efficiency over a wide range. The efficiency is measured to be 50% at 100 cm, which corresponds to a 46% increase compared to a conventional WPT system without the loop switching technique.

1. INTRODUCTION

Recently, there has been increasing interest in WPT for various applications such as wireless charging and space solar power satellites. Three types of WPT techniques have been reported: EM radiation using propagating waves, inductive coupling, and magnetic resonance coupling [1]. In the EM radiation technique, a highly directional antenna is used to transmit and receive microwave energy from point to point, allowing power transmission over long distances (kilometer range). However, it generally exhibits low efficiency due to loss in air and misalignment between the transmit and receive antennas. In addition, EM radiation is known to be harmful to the human

Received 21 January 2013, Accepted 15 March 2013, Scheduled 20 March 2013

* Corresponding author: Jinho Jeong (jjeong@sogang.ac.kr).

body [2, 3]. Inductive coupling is a well-known WPT technique that has been widely used in wireless charging applications, such as electric toothbrushes, cell phones, laptops and electrical vehicles. Since this method is based on magnetic coupling between two close coils, its operating range is limited to short-distances less than a centimeter [4].

The magnetic resonance coupling technique can extend the operating range to longer distances, in the range of tens of centimeters to a few meters, utilizing evanescent-wave coupling between two resonant coils [5–9]. However, there exists an optimum distance between the transmit and receive coils for maximum efficiency. Unfortunately, the efficiency rapidly decreases if the distance deviates from the optimum value. Therefore, there have been several studies on maintaining high efficiency over a wide range, or range adaptation techniques. In one study, the distance between the source and transmit coils was manually changed to vary the coupling coefficient according to the distance between the transmit and receive coils [10]. This allowed the efficiency to increase for long distances. However, the manual tuning requires equipment such as motors in real applications, which complicates the system and dissipates additional power. Frequency tuning has been carried out to mitigate the frequency splitting effect and to obtain high efficiency at close distances [11]. The drawback of this method is that it requires a wide operating bandwidth for the WPT systems. Tunable impedance matching was proposed to improve the efficiency with distance [12]. However, the tuning range was limited by the varactors used in the matching circuit, which also reduced the total efficiency due to varactor losses.

We propose a loop switching technique to maintain high efficiency over a wide operating range. In this technique, one of several loops with different sizes is selected to adjust the coupling coefficient such that the optimum efficiency can be achieved, depending on the distance. In Section 2, we present an overview and analysis of the conventional magnetic resonance coupling WPT system. The proposed loop switching technique is explained in Section 3 with EM and circuit analyses. The design of a 13.56-MHz WPT system is also discussed. Finally, the experimental results of a fabricated WPT system are presented in the Section 4.

2. WPT SYSTEM USING MAGNETIC RESONANCE COUPLING

2.1. Design Principle

Figure 1 shows a schematic of a previously proposed WPT system using four magnetically coupled resonators [6]. The power in the

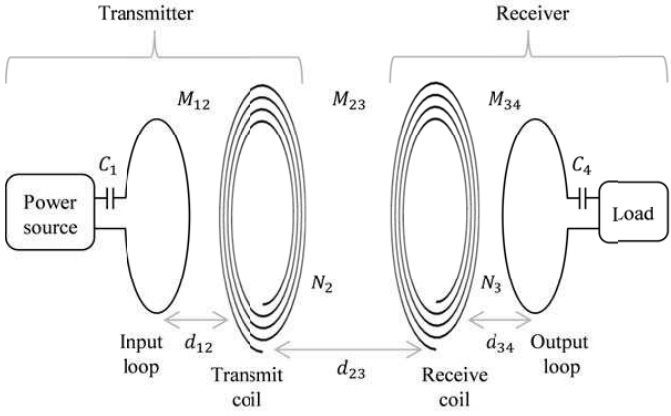

Figure 1. WPT system using magnetic resonance coupling.

input loop with a single turn is magnetically coupled to an N_2-turn transmit coil by mutual inductance M_{12}. The power stored in the transmit coil is transferred to an N_3-turn receive coil. M_{23} represents the mutual inductance between the transmit and receive coils. Finally, the power is delivered to the output loop and the load. For maximum power transfer, four resonators are designed to have the same resonant frequency. In this WPT system, the power transfer efficiency is strongly dependent on the distance d_{23} between the transmit and receive coils. Therefore, there exists an optimum d_{23} to allow maximum efficiency for the system. The efficiency rapidly decreases at distances deviating from the optimum d_{23}. This is the main problem that we try to solve in this paper.

2.2. Analysis

For the analysis, the WPT system shown in Figure 1 is modeled by the equivalent circuit given in Figure 2. L_i and R_i represent the self-inductance and parasitic resistance of the loops and coils ($i = 1 \sim 4$). The external capacitors C_1 and C_4 are connected to the input and output loops to resonate with L_1 and L_4, respectively. C_2 and C_3 are the parasitic capacitances of the transmit and receive coils, which are also respectively resonant with L_2 and L_3. The adjacent two inductors are magnetically coupled by mutual inductances (M_{12}, M_{23}, and M_{34}). The cross couplings between non-adjacent inductors are neglected, with $M_{13} = M_{14} = M_{24} = 0$. The power source is represented by the voltage source V_s and source resistor R_s. The load resistance is denoted by R_L.

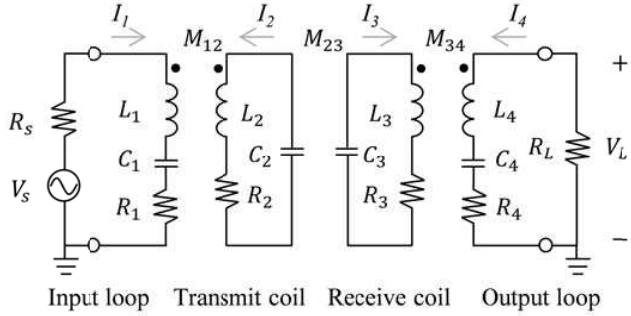

Figure 2. Equivalent circuit of the WPT system.

By applying Kirchhoff's voltage law (KVL), we obtain the following four equations regarding currents ($I_1 \sim I_4$) and voltage (V_s),

$$\begin{aligned}
\left(R_s + R_1 + j\omega L_1 + \frac{1}{j\omega C_1}\right) I_1 + j\omega M_{12} I_2 &= V_s \\
\left(R_2 + j\omega L_2 + \frac{1}{j\omega C_2}\right) I_2 + j\omega (M_{12} I_1 + M_{23} I_3) &= 0 \\
\left(R_3 + j\omega L_3 + \frac{1}{j\omega C_3}\right) I_3 + j\omega (M_{34} I_4 + M_{23} I_2) &= 0 \\
\left(R_L + R_4 + j\omega L_4 + \frac{1}{j\omega C_4}\right) I_4 + j\omega M_{34} I_3 &= 0
\end{aligned} \tag{1}$$

where ω is an angular frequency in rad/s. For the resonators with high-quality (Q)-factors, $R_1 \ll R_s$ and $R_4 \ll R_L$. Therefore, $R_s + R_1 \approx R_s$ and $R_L + R_4 \approx R_L$. At resonant frequency, $\omega_0 = 1/\sqrt{L_i C_i}$, $(i = 1 \sim 4)$, each current can be obtained as:

$$\begin{bmatrix} I_1 \\ I_2 \\ I_3 \\ I_4 \end{bmatrix} = \begin{bmatrix} R_s & j\omega_0 M_{12} & 0 & 0 \\ j\omega_0 M_{12} & R_2 & j\omega_0 M_{23} & 0 \\ 0 & j\omega_0 M_{23} & R_3 & j\omega_0 M_{34} \\ 0 & 0 & j\omega_0 M_{34} & R_L \end{bmatrix}^{-1} \begin{bmatrix} V_s \\ 0 \\ 0 \\ 0 \end{bmatrix} \tag{2}$$

For the simplicity of the analysis, we assume that the system is symmetrical, with input loop and transmit coil identical to the output loop and receive coil, respectively. As such, $L_1 = L_4$, $L_2 = L_3$, $R_1 = R_4$, $R_2 = R_3$, $C_1 = C_4$, and $C_2 = C_3$. In addition, $R_s = R_L = R_0$. The quality factor of each resonator is as follows: $Q_1 = Q_4 = \omega L_1/R_0$, $Q_2 = Q_3 = \omega L_2/R_2$. The coupling coefficient k_{12} is equal to k_{34}, k_{ij} where is $M_{ij}/\sqrt{L_i L_j}$.

Finally, we can determine the power transfer efficiency η, which is defined as the power delivered to the load divided by the maximum power available from the source [11] as follows:

$$\eta = \frac{V_L^2/R_L}{V_s^2/4R_s} = \left[\frac{2k_{23}k_{12}^2Q_1Q_2^2}{(1+k_{12}^2Q_1Q_2)^2 + k_{23}^2Q_2^2}\right]^2 \tag{3}$$

By definition, the efficiency in (3) is equal to transducer power gain of a two-port network, or scattering parameter ($|S_{21}|^2$), which can be measured by a network analyzer [13]. This equation implies that the efficiency is influenced by the coupling coefficients, k_{12} and k_{23}, for a given Q_1 and Q_2. The coupling coefficient k_{23} is a strong function of the distance d_{23}. Using the Neumann formula, the mutual inductance between two symmetrical coils with N turns and a radius of r can be approximated for the case of $r \ll d_{23}$ as:

$$M_{23} \cong \frac{\mu_0 \pi N^2 r^4}{2d_{23}^3} \tag{4}$$

where μ_0 is the permeability of free space [10]. Therefore, the relation between k_{23} and d_{23} can be derived as:

$$k_{23} \cong \frac{\mu_0 \pi N^2 r^4}{2Ld_{23}^3} \tag{5}$$

where L is a self-inductance of each coil, or $L = L_2 = L_3$ for the symmetric coils. It can be found from this equation that k_{23} is proportional to $1/d_{23}^3$, such that the efficiency in (3) dramatically decreases with the distance d_{23}.

The efficiency can be maximized for a given k_{23} (or d_{23}) by choosing an optimum k_{12} such that:

$$\frac{\partial \eta}{\partial k_{12}} = 0 \quad \text{at} \quad k_{12} = k_{12,opt} \tag{6}$$

From this equation, $k_{12,opt}$ and the optimum efficiency η_{opt} are determined as:

$$k_{12,opt} = \sqrt[4]{\frac{1}{Q_1}k_{23}^2 + \frac{1}{Q_1^2Q_2^2}} \tag{7}$$

$$\eta_{opt} = \left(\frac{2Q_2k_{23}\sqrt{Q_1^2Q_2k_{23}^2+1}}{\left(\sqrt{Q_1Q_2^2k_{23}^2+1}+1\right)^2 + Q_2^2k_{23}^2}\right)^2 \tag{8}$$

In summary, optimum efficiency can be achieved with the distance d_{23}, if the coupling coefficient k_{12} can be adjusted to satisfy Equation (7). According to Neumann's formula (4), the coupling coefficient can be controlled by the distance between two coils, the number of turns, and the radius of the coils.

3. PROPOSED WPT SYSTEM

3.1. Loop Switching Technique

We propose the loop switching technique adjusting k_{12} with the distance d_{23} close to $k_{12,opt}$. This range adaptation results in high efficiency over a distance. Figure 3 shows the WPT system using the loop switching technique, with input and output loops that consist of four loops with different radii. The power source and load are switched to one of the four loops according to the distance d_{23}. For example, the largest loop 1 is connected for the shortest d_{23}. The loops 2, 3, and 4 are connected in order as the distance increases. This loop switching allows the adjustment of coupling coefficient k_{12}, providing high efficiency with d_{23}.

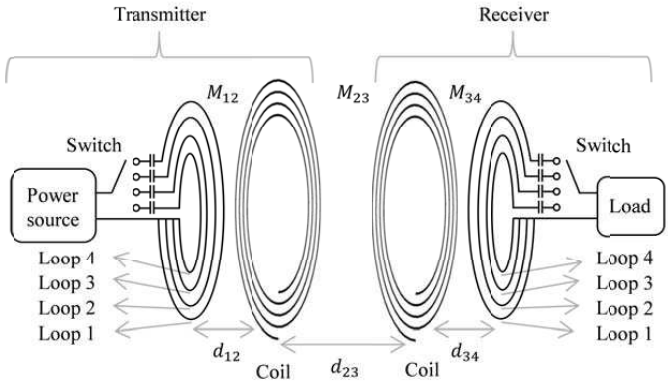

Figure 3. Proposed loop switching WPT system.

3.2. Design of the Proposed WPT System

We design the proposed WPT system with four loops depicted in Figure 3, with symmetrical transmitter and receiver. Each loop has a series-connected capacitor to provide the same resonant frequency of 13.56 MHz. The coils are carefully designed for the self-inductance and parasitic capacitance to resonate at ω_0. The dimensions of the designed loops and coils are provided in Table 1. They are fabricated using copper wire with a diameter of 0.3 cm. The loops are placed close to the coils with a spacing of $d_{12} = d_{34} = 0.5$ cm.

Table 2 shows the simulated and measured electrical parameters of the designed loops and coils. The simulation is performed by ANSYS HFSS version 11, which is a full-wave EM solver based on finite element method. A vector network analyzer is used to obtain

Table 1. Dimensions of the designed loops and coils.

	Number of turns	Outer diameter (cm)	Inner diameter (cm)	Pitch (cm)	Wire diameter (cm)
Coil	4	68.0	45.0	3.0	0.3
Loop 1	1	33.0	–	–	0.3
Loop 2	1	28.0	–	–	0.3
Loop 3	1	23.5	–	–	0.3
Loop 4	1	19.0	–	–	0.3

Table 2. Simulated and measured electrical parameters of loops and coils.

		Inductance (μH)	Resistance (Ω)	Resonant frequency (MHz)	Q-factor at resonant frequency
Coil	Simulation	15.91	1.20	13.56	1130
	Measurement	15.70	3.20	13.55	418
Loop 1	Simulation	1.10	0.15	13.56	625
	Measurement	1.27	0.51	13.60	213
Loop 2	Simulation	1.02	0.15	13.56	599
	Measurement	1.11	0.45	13.70	212
Loop 3	Simulation	0.89	0.14	13.56	546
	Measurement	0.96	0.39	13.70	212
Loop 4	Simulation	0.80	0.13	13.56	516
	Measurement	0.85	0.35	13.60	208

measured data. The inductance and resonant frequency of the coils are extracted by examining the imaginary part of the impedance versus frequency. Based on the extracted inductance and resonant frequency, the capacitance of the coils is computed from $\omega_0 = 1/\sqrt{LC}$. It is challenging to determine the parasitic resistance of the resonator with high Q-factor, since its impedance steeply varies around the resonant frequency. In this work, the fabricated coil is unwound to minimize the parasitic capacitance, so that the resonance disappears. Then, S-parameters of the non-resonant straight copper wire are measured. Finally, the resistance is determined from the real part of the impedance converted from the S-parameters. The electrical parameters of the loops are determined in a similar manner.

As shown in Table 2, the designed loops and coils exhibit almost the same resonant frequency, which is critical for achieving high efficiency in a WPT system. The measured Q-factor of the coils is about 418, which is higher than values reported previously in [10, 11]. One of the reasons for higher Q-factor seems to be a higher resonant frequency adopted in this work [16]. The fabricated loops show a Q-factor of around 210. The extracted inductance and resonant frequency show good agreement between the simulation and measurement. The substantial discrepancy in the resistance is because the real wire exhibits a higher resistance due to the poorly conducting oxide layer on the copper surface [6]. This effect is not included in the EM simulation.

3.3. Simulation Results

The power transfer efficiency is a strong function of the distance d_{23}, as predicted in (3). In the proposed WPT system, one of the four loops is connected to the source (and load) depending on d_{23}, such that k_{12} satisfies Equation (7). Therefore, for the design of the proposed WPT system, k_{23} and the corresponding $k_{12,opt}$ should be calculated as a function of d_{23}. Equation (4) is an approximated Neumann's formula for long distances of $r \ll d_{23}$. Thus, the original Neumann's formula should be used to accurately predict $k_{12,opt}$ at any distance.

First, we can compute the mutual inductance M_{mn} between two single-turn loop m and n using the Neumann formula as follows [14, 15]:

$$M_{mn} = \frac{\mu_0}{4\pi} \oint_m \oint_n \frac{\vec{dl_m} \cdot \vec{dl_n}}{r} \tag{9}$$

where μ_0 is the permittivity of free space, and r is the distance between the incremental lines $\vec{dl_m}$ and $\vec{dl_n}$ on the respective loop m and n. In order to determine the total mutual inductance M_{total} between two coils with N_1 and N_2 turns, two coils are decomposed into the sets of N_1 and N_2 closed loops. Then, M_{total} is approximated as the sum of the mutual inductances M_{mn} between the loops m and n as follows

$$M_{total} = \sum_{m=1}^{N_1} \sum_{n=1}^{N_2} M_{mn} \tag{10}$$

Figure 4 presents the computed k_{23} as a function of d_{23} based on Equations (9) and (10) using the dimensions in Table 1. The corresponding is also calculated using Equation (7). The computed for each loop with the dimensions in Table 1 is plotted as a function of the targeted d_{23} point. Loop 1 is targeted for $d_{23} = 30\,\text{cm}$, loop 2 for $d_{23} = 50\,\text{cm}$, loop 3 for $d_{23} = 70\,\text{cm}$, and loop 4 for $d_{23} = 90\,\text{cm}$. This figure validates that the proposed loop switching technique can

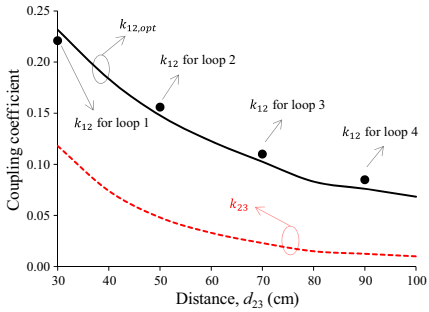

Figure 4. Computed k_{23} (dashed line) and $k_{(12,opt)}$ (solid line) as a function of d_{23} of the designed WPT systems with dimensions in Table 1. The k_{12} (dot) for each loop is also plotted.

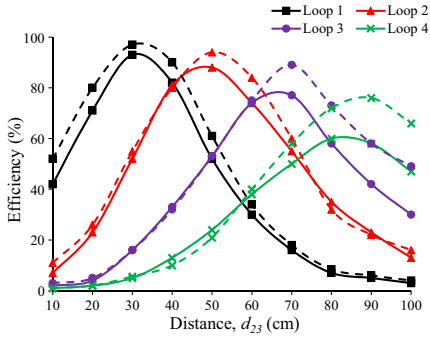

Figure 5. Simulated power transfer efficiency of the designed WPT system at 13.56 MHz. Dashed lines: EM simulation; solid lines: circuit simulation.

provide an adjustable k_{12} close to $k_{12,opt}$ depending on d_{23}, providing range adaptation to allow high efficiency over a wide range of distances.

EM and circuit simulations are carried out to predict the power transfer efficiency of the proposed WPT system. ANSYS HFSS was used for the EM simulation with the dimensions in Table 1. The circuit simulation was performed using the extracted R, L, C, values from the measurement in Table 2 and the coupling coefficients in Figure 4. Agilent ADS 2011 was used for the circuit simulation. Figure 5 shows the simulated efficiency at 13.56 MHz as a function of the distance d_{23}. This figure indicates that one of the four loops can be selected to obtain high efficiency depending on the distance d_{23}: loop 1 for d_{23} less than 42 cm, loop 2 for d_{23} from 42 to 61 cm, loop 3 for d_{23} from 61 to 80 cm, and loop 4 for d_{23} greater than 80 cm. This simulation result clearly shows that the proposed loop switching technique enables the WPT system to maintain high efficiency along the distances. The efficiency difference between the EM and circuit simulations is due to the underestimated parasitic resistance in EM simulation.

4. EXPERIMENTAL RESULTS

The designed WPT system was fabricated as shown in Figure 6. The S-parameters of the fabricated WPT system were measured using a vector network analyzer. Figure 7 shows the measured power transfer efficiency at 13.56 MHz as a function of the distance d_{23}. In the

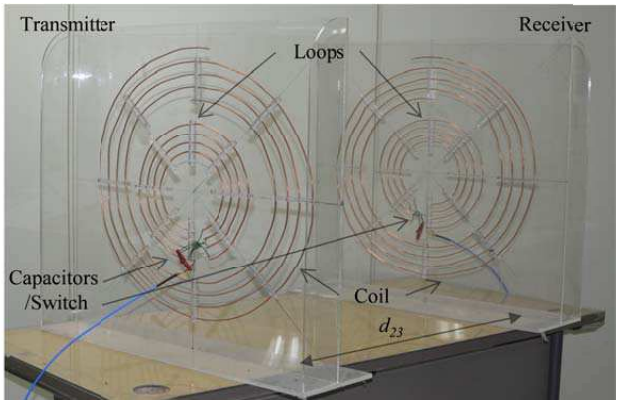

Figure 6. Photograph of the fabricated WPT system.

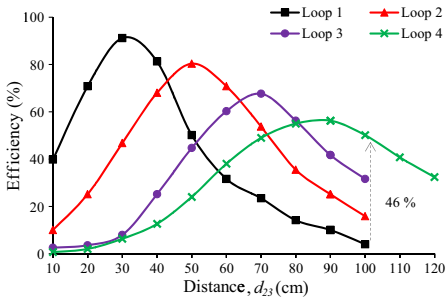

Figure 7. The measured efficiency of the proposed WPT system at 13.56 MHz.

results, the proposed system achieves a maximum efficiency of 91% at $d_{23} = 30$ cm (loop 1 selected) and 50% at $d_{23} = 100$ cm (loop 4 selected). If loop 1 is connected, the system shows only 4% efficiency at $d_{23} = 100$ cm. Switching to loop 4 increases the efficiency by 46% at the same distance, which proves the excellence of the proposed technique. This measurement result implies that one of the loops can be selected to maximize the efficiency according to the distance. That is, the system can switch from loop 1 to loop 2, loop 3, and loop 4 as the distance increases.

At a short distance ($d_{23} < 42$ cm), loop 1 is selected, and the peak efficiency is over 90%. However, the efficiency rapidly decreases as the distance deviates from the peak points (for example, $d_{23} = 30$ cm for loop 1). At $d_{23} < 30$ cm, the efficiency decreases due to the frequency splitting effect [11]. Efficiency drops are also found at mid-distance

between two selected loops, for example, at 40 cm, between loop 1 and loop 2.

These efficiency drops can be minimized by employing more loops or variable impedance matching circuits. Another remedy is to adjust the input frequency at the distance closer than the critical coupling point where the transmit and receive coils are over-coupled and frequency splitting is occurred [11]. To recover efficiency at the close distances, the input frequency was adjusted in the range of 10.6 and 13.56 MHz for each loop. For example, for the loop 1, the measurement frequency was varied for maximum efficiency at $d_{23} < 30$ cm, while it was fixed to 13.56 MHz at $d_{23} \geq 30$ cm. The measurement result is shown in Figure 8. The efficiency was increased from 49% to 89% at d_{23} of 10 cm by using the frequency adjustment. This measurement result indicates that the frequency adjustment can eliminate the efficiency drops and maintain high efficiency along the distance.

For comparison, the measured data from previous studies are also included in Figure 8 [10, 11]. One previous result used the resonant frequency of 6.7 MHz [10], compared to which the proposed system accomplishes higher efficiency over a long distance due to higher-Q-factor resonators [16]. Another WPT system designed to have high efficiency over a long distance shows low efficiency at close distances, even though frequency adjustment was carried out to avoid the frequency splitting effect [11]. This is due to the fact that the critical coupling point is determined by k_{12} and was fixed to small value in [11] to obtain high efficiency at long distance at the cost of the short-distance efficiency. In contrast, the loop switching in this work allows the adjustment of k_{12} and critical point according to the distance, resulting in high efficiency across a wide range of distances.

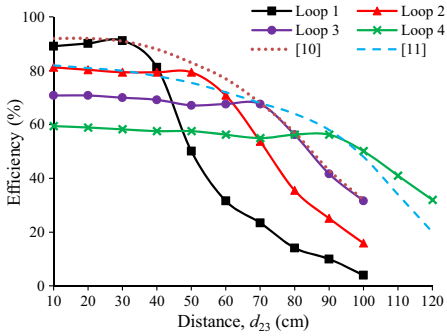

Figure 8. The measured efficiency of the proposed WPT system. The measurement frequency was adjusted for maximum efficiency at the distance closer than the critical coupling point of each loop.

5. CONCLUSION

We have proposed a loop switching technique to improve the efficiency of a WPT system using magnetic resonance coupling. From the analysis, it was shown that there existed an optimum coupling coefficient $k_{12,opt}$ that allowed maximum efficiency as a function of the coupling coefficient k_{23}, which was varied with the distance and orientation of the coils. The proposed loop switching technique employed several loops with different sizes, which allowed the adjustment of the coupling coefficient. One of the loops was selected depending on k_{23} or the distance, in order to optimize the efficiency. The measurement proved that the proposed WPT system maintained high efficiency across a wide range of distances.

ACKNOWLEDGMENT

This research was supported by Basic Science Research Program through the National Research Foundation of Korea (NRF) funded by the Ministry of Education, Science and Technology (2012R1A1B3000836).

REFERENCES

1. Wei, X. C. and E. P. Li, "Simulation and experimental comparison of different coupling mechanisms for the wireless electricity transfer," *Journal of Electromagnetic Waves and Applications*, Vol. 23, No. 7, 925–934, 2009.
2. Sim, Z. W., R. Shuttleworth, M. J. Alexander, and B. D. Grieve, "Compact patch antenna design for outdoor RF energy harvesting in wireless sensor networks," *Progress In Electromagnetics Research*, Vol. 105, 273–294, 2010.
3. Yu, C, C.-J. Liu, B. Zhang, X. Chen, and K.-M. Huang, "An intermodulation recycling rectifier for microwave power transmission at 2.45 GHz," *Progress In Electromagnetics Research*, Vol. 119, 435–447, 2011.
4. Ravaud, R., G. Lemarquand, V. Lemarguand, S. I. Babic, and C. Akyel, "Mutual inductance and force exerted between thick coils," *Progress In Electromagnetics Research*, Vol. 102, 367–380, 2010.
5. Karalis, A., J. Joannopoulos, and M. Soljacic, "Efficient wireless non-radiative mid-range energy transfer," *Annals of Physics*, Vol. 323, No. 1, 34–48, 2008.

6. Kurs, A., A. Karalis, R. Moffatt, J. D. Joannopoulos, P. Fisher, and M. Soljacic, "Wireless power transfer via strongly coupled magnetic resonances," *Science*, Vol. 317, No. 5834, 83–86, Jul. 2007.
7. Cannon, B., J. Hoburg, D. Stancil, and S. Goldstein, "Magnetic resonant coupling as a potential means for wireless power transfer to multiple small receivers," *IEEE Transactions on Power Electronics*, Vol. 24, No. 7, 1819–1825, Jul. 2009.
8. Low, Z. N., R. Chinga, R. Tseng, and J. Lin, "Design and test of a high-power high-efficiency loosely coupled planar wireless power transfer system," *IEEE Transactions on Industrial Electronics*, Vol. 56, No. 5, 1801–1812, May 2009.
9. Casanova, J., Z. N. Low, and J. Lin, "A loosely coupled planar wireless power system for multiple receivers," *IEEE Transactions on Industrial Electronics*, Vol. 56, No. 8, 3060–3068, Aug. 2009.
10. Duong, T. P. and J.-W. Lee, "Experimental results of high-efficiency resonant coupling wireless power transfer using a variable coupling method," *IEEE Microwave and Wireless Components Letters*, Vol. 21, No. 8, 442–444, Aug. 2011.
11. Sample, A. P., D. A. Meyer, and J. R. Smith, "Analysis, experimental results, and range adaptation of magnetically coupled resonators for wireless power transfer," *IEEE Transactions on Industrial Electronics*, Vol. 58, No. 2, 544–554, Feb. 2011.
12. Jang, B.-J., S. Lee, and H. Yoon, "HF-band wireless power transfer system: Concept, issues, and design," *Progress In Electromagnetics Research*, Vol. 124, 211–231, Jan. 2012.
13. Barroso, J. J. and A. L. de Paula, "Retrieval of permittivity and permeability of homogeneous materials from scattering parameters," *Journal of Electromagnetic Waves and Applications*, Vol. 24, Nos. 11–12, 1563–1574, 2010.
14. Lee, W.-S., H. L. Lee, K.-S. Oh, and J.-W. Yu, "Switchable distance-based impedance matching networks for tunable HF system," *Progress In Electromagnetics Research*, Vol. 128, 19–34, 2012.
15. Akyel, C., S. I. Babic, and M.-M. Mahmoudi, "Mutual inductance calculation for non-coaxial circular air coils with parallel axes," *Progress In Electromagnetics Research*, Vol. 91, 287–301, 2009.
16. Kuhn, W. B. and N. M. Ibrahim, "Analysis of current crowding effects in multiturn spiral inductors," *IEEE Transactions on Microwave Theory and Techniques*, Vol. 49, No. 1, 31–38, Jan. 2001.